Available online at www.sciencedirect.com
ScienceDirect
Trans. Nonferrous Met. Soc. China 28(2018) 1192−1199
Transactions of Nonferrous Metals Society of China
www.tnmsc.cn

Atomistic simulations of interactions between screw dislocation and twin boundaries in zirconium

Xiao-zhi TANG, Hui-shi ZHANG, Ya-fang GUO

Institute of Engineering Mechanics, Beijing Jiaotong University, Beijing 100044, China

Received 21 January 2017; accepted 18 July 2017

Abstract: Molecular statics was employed to simulate interaction between screw dislocation and twin boundaries (TB) in hexagonal close-packed zirconium. In the moving TB model, the interaction of a moving $\{10\bar{1}2\}$ TB with a static $1/3\langle 11\bar{2}0\rangle\{10\bar{1}0\}$ screw dislocation was investigated. Twinning dislocation (TD) nucleation and movement play an important role in the interaction. The screw dislocation passes through the moving TB and changes to a basal one with a wide core. In the moving dislocation model, a moving $1/3\langle 11\bar{2}0\rangle\{10\bar{1}0\}$ dislocation passes through the TB, converting into a basal one containing two partial dislocations and an extremely short stacking fault. If the TB changes to the $\{10\bar{1}1\}$ one, the moving $1/3\langle 11\bar{2}0\rangle\{10\bar{1}0\}$ prismatic screw dislocation can be absorbed by the static TB and dissociated into two TDs on the TB. Along with the stress−strain relationship, results reveal the complicated mechanisms of interactions between the dislocation and TBs.

Key words: twin boundary; twinning dislocation; slip transfer reaction; athermal process

1 Introduction

Interaction between dislocation and grain boundary (GB) has the most significant influence on the mechanical properties of polycrystalline metals [1]. In face-centered cubic (fcc) metals, such as copper, GB-dislocation reaction leads to the increasing yield strength with the decreasing average gain size due to dislocation pile-up at the interface [2,3], namely the Hall−Petch relation [4,5], or grain-boundary strengthening. When grain size downgrades below 100 nm, nanocrystalline brings out a bright future on its application with excellent mechanical properties [6,7], especially due to the effect of GB−dislocation interaction at the nanoscale. Generally speaking, twin boundary (TB) is a special interface which usually introduces slip transfer [8] or interface defect [9] rather than the conspicuous dislocation pile-up mechanism. Comparing with other general non-coherent interfaces, TB is geometrically favorable for the slip transfer [10−13].

Therefore, the mechanism of TB−dislocation interaction is thought to be somewhat different from that of general GB−dislocation interaction. Whether the dislocation is transited, absorbed, or even desorbed by the interface, TB−dislocation interaction is strongly related to bulk plasticity and plays an important role in the kinetic process of mechanical properties of materials.

In hexagonal close-packed (hcp) metals, twinning is the dominant deformation mechanism due to the limited number of slip systems compared with fcc or body-centered cubic (bcc) metals. TB−dislocation interactions in hcp structure are now receiving more and more attention [14]. There are experiment and simulation works on dislocation−interface interactions in titanium, magnesium and other hcp metals [15−24] by electron microscopy, dislocation dynamics (DD), and molecular dynamics (MD). For example, KASCHNER et al [15] explored dislocation−twin interactions in zirconium. Their transmission electron microscopy (TEM) result revealed that twins play a dominant role in determining the hardening. In 2014, in-situ straining TEM and diffraction-contrast electron tomography have been applied to investigating dislocation−GB and dislocation−TB interactions in α-Ti. It was found that, the transfer of dislocations across GBs is governed primarily by the minimization of the magnitude of the Burgers vector of the residual grain boundary dislocation [16]. By MD simulation, SERRA et al [18,19] revealed the interaction mechanisms of matrix screw dislocations with TBs in

Foundation item: Projects (11372032, 11602015) supported by the National Natural Science Foundation of China
Corresponding author: Ya-fang GUO; Tel: +86-10-51682094; E-mail: yfguo@bjtu.edu.cn
DOI: 10.1016/S1003-6326(18)64757-0

α-Ti and magnesium. They revealed that the screw dislocation crosses the $\{10\bar{1}2\}$ TB by cross-slip, but the $\{10\bar{1}1\}$ TB usually absorbs the screw by a process of decomposition into two twinning dislocations (TDs). Then, SERRA and BACON [20] claimed that the screw dislocation does not decompose in a moving $\{10\bar{1}2\}$ TB, while the 60°-mixed dislocation is attracted by the boundary and decomposes into TDs. YUASA et al [21] published their MD work in magnesium which reported that the screw partials are absorbed readily in the $\{10\bar{1}1\}$ TB. Moreover, ZHANG et al [22] reported their TEM work in titanium [22], which showed that the dissociation of non-screw dislocation into different Frank partial dislocations on the $\{10\bar{1}2\}$ interfacial plane is more favorable than the transmission to the other side of the interface. The formation of the Frank partials at the TB can produce a small change in the TB misorientation angle. Very recently, the interactions between basal dislocation and TB were used to explain the profuse existence of $\{10\bar{1}2\}$ twins in magnesium [23]. Both $\{10\bar{1}2\}$ and $\{10\bar{1}1\}$ TBs interacting with screw partial dislocations in pure Mg and Mg−Y alloy were investigated [24]. Results showed that $\{10\bar{1}2\}$ TB is easy to be passed through by the screw partial, while $\{10\bar{1}1\}$ brings more complex behaviors.

Based on the analysis above, it is found that the mechanisms of GB/TB−dislocation interactions are complicated and need further clarification on various interface-slip systems. In our work, atomistic simulations are applied to giving detailed description on interactions of two commonly reported TBs in hcp metals [22] separately with a screw dislocation. We focus on different mechanical properties as well as atomic configuration change in these interactions.

2 Simulation methods

Two modeling systems for TB−dislocation interactions are established in Fig. 1. The first one in Fig. 1(a) is a TB moving toward the screw dislocation under a shear strain imposed parallel to the twin interface. In Fig. 1(b), the TB is kept still, while the screw dislocation moves toward the static TB by applying the shear strain parallel to Burgers vectors of the dislocation. Atoms at the intersection places where the boundary meets the free surface are fixed during energy minimization to keep the interface structure integrity. For the moving TB model in Fig. 1(a), a moving $\{10\bar{1}2\}$ TB is selected to interact with a static $1/3\langle 11\bar{2}0\rangle\{10\bar{1}0\}$ prismatic screw dislocation. While for the moving dislocation model in Fig. 1(b), the moving $1/3\langle 11\bar{2}0\rangle\{10\bar{1}0\}$ prismatic screw dislocation is selected to interact with $\{10\bar{1}2\}$ and $\{10\bar{1}1\}$ TBs, separately. The periodic boundary condition (PBC) is applied along the dislocation line direction, and the twin plane is parallel to dislocation lines of screw dislocations. Shear strain is discretely introduced into system by incremental displacements of the moving rigid body (shown in yellow). After each incremental displacement, system was relaxed by minimizing potential energy using the interatomic potential for Zr provided by MENDELEV and ACKLAND [25]. Since equivalence may hold between molecular statics (MS) and molecular dynamics for strain rates less than 10^8 s^{-1} at low temperatures [26], our simulation results obtained from this discrete-strain based methodology could be considered as dynamic simulation without thermal activation processes.

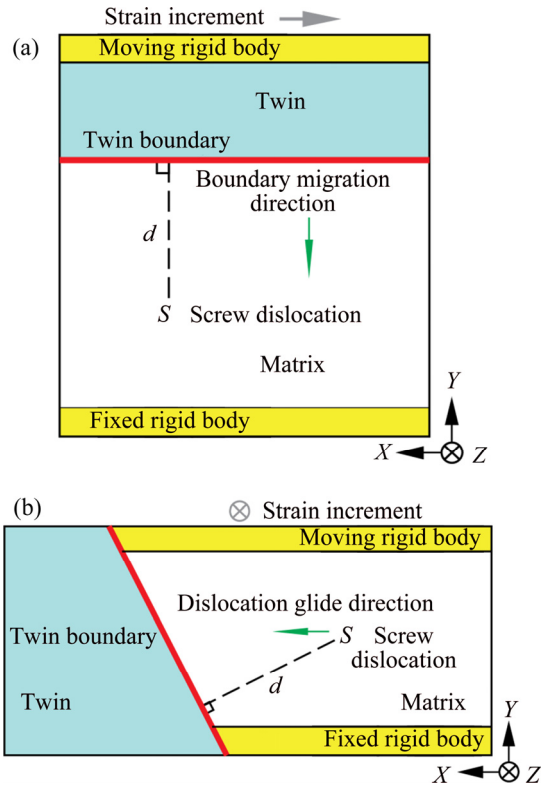

Fig. 1 Schematics of moving TB model (a) and moving dislocation model (b)

The $\{10\bar{1}2\}$ and $\{10\bar{1}1\}$ TBs are constructed according to Refs. [15,16,18,27]. To construct a GB, atoms in the matrix and the twin region are initially created with symmetric lattice orientation, and then, those atoms in the contact region of two grains within a specified cutoff distance were deleted. A following rigid-body translation in all three Cartesian directions was applied to seeking the stable structure. The whole system was relaxed to ground state by MS method to get the lowest grain boundary energy. The calculated twin boundary energy using current atomic potential is 330 mJ/m^2 for $\{10\bar{1}2\}$ type and 215 mJ/m^2 for $\{10\bar{1}1\}$ type separately (comparing with 262 mJ/m^2 and 225 mJ/m^2 in Ref. [28] using a different potential). The

models we used for each simulation are slightly different in size. Roughly speaking, the models are around 75 nm × 100 nm × 2.5 nm in three dimensions, and the shortest one is in the PBC direction.

3 Results

3.1 Interaction between moving {10$\bar{1}$2} TB and static 1/3⟨11$\bar{2}$0⟩{10$\bar{1}$0} prismatic screw dislocation

The model with a moving {10$\bar{1}$2} TB and a static 1/3⟨11$\bar{2}$0⟩{10$\bar{1}$0} prismatic screw dislocation is established in Fig. 1(a). As shown in Fig. 2, when the applied strain is below 2.5%, the stress increases linearly with the strain, and the whole system is under an elastic response. When the strain is beyond 2.5%, the TB begins to move, indicated by the fluctuation of the plastic flow stress. The free move of TB is accomplished by the nucleation, gliding and escape of TD dipole in this modeling system. Under the applied shear strain, TD dipoles nucleate spontaneously on the TB, and then the two TDs in each dipole glide in the opposite directions to the free surfaces and escape from them. When the TB moves close to the dislocation (*B*), the intersection point of the prismatic plane and the interface becomes the nucleation site of TDs. After two new TDs (one dipole) formed at this site and glided separately in opposite directions (*C*), the twin interface and the dislocation are attached together. The TB is pinned here along with a linear increase of the shear stress of about 0.04 GPa, then it touches dislocation core. The stress increase in this process shows that the screw dislocation plays as an obstacle to the TB migration.

Subsequently, there are three individual TDs involved in the further interaction process. From (*C*) to (*D*), the strain keeps growing of approximately 0.3% without any change of atomic configuration, until the first TD dipole nucleates near the dislocation core and then one TD moves towards the screw dislocation and interacts with it (*D*). It is observed that the interaction between the TD and the dislocation totally changed the geometric character of dislocation (*E*), converting the original prismatic screw dislocation to a basal one on the

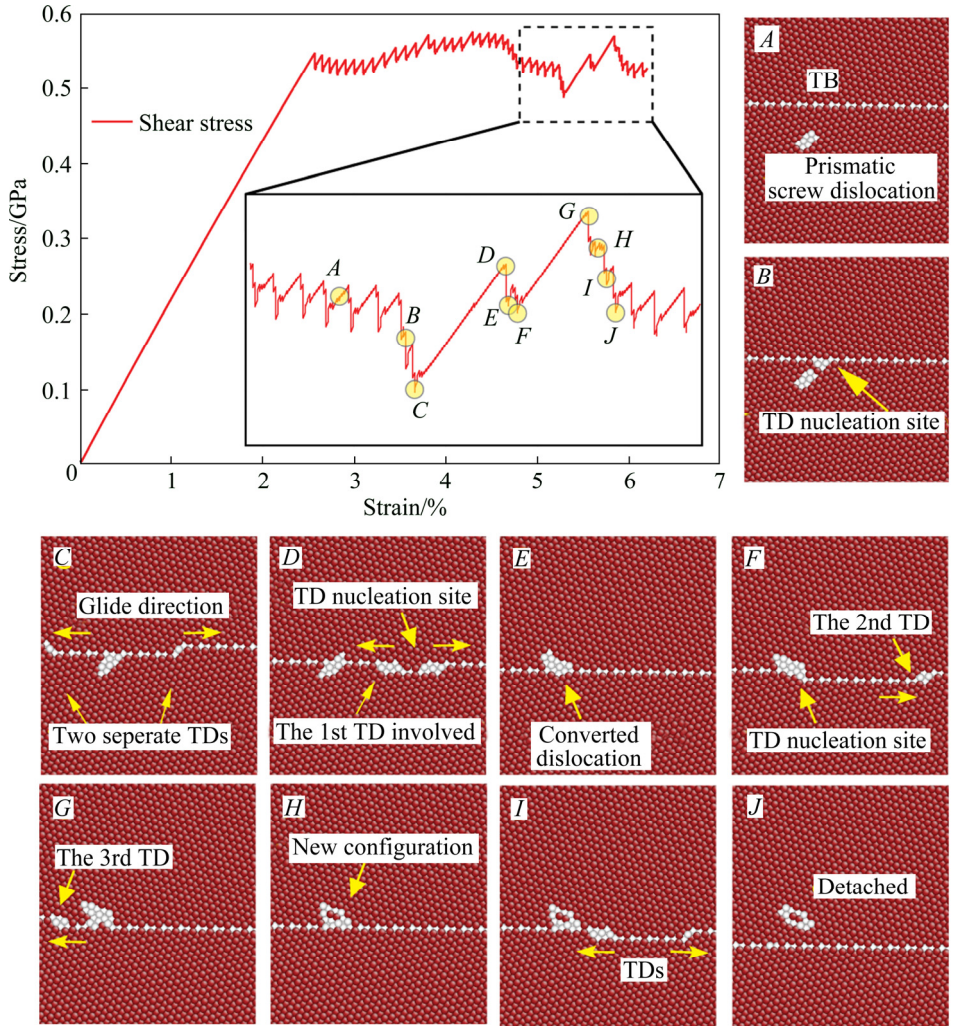

Fig. 2 Stress−strain curve and corresponding atomic configurations of moving {10$\bar{1}$2} TB interacting with static 1/3⟨11$\bar{2}$0⟩{10$\bar{1}$0} prismatic screw dislocation (*A*−*J*)

other side of the twin interface. Soon afterwards in *F*, the second TD nucleates at the site where the basal screw dislocation located, and moves to the right shortly. After the minor stress decreases due to the nucleation and movement of these two TDs, system maintained the configuration in *F* for 0.3% strain increasing, accompanied by an increase of stress from 0.04 GPa to its peak of 0.57 GPa. In *G*, the third TD nucleates and moves to the left side of the TB, and the dislocation converts to its final configuration, which is still a basal defect on the TB (*H*) with a screw component of $1/3\langle 11\bar{2}0\rangle$, same as the static dislocation before the interaction. According to Ref. [29], the TD on $\{10\bar{1}2\}$ TB only has a Burgers vector of $\lambda\langle 10\bar{1}1\rangle$, where λ is 0.0883 using the current potential, but does not affect the Burgers vector balancing. This is because all the three involved TDs remain their Burgers vectors, and the Burgers circuit check around the defect straightly proves that there is no edge component in the product. The basal screw dislocation does not show mobility under current shear stress along the $\{10\bar{1}1\}$ direction. At the strain of about 6%, the line defect is finally detached from the moving TB (*J*), accompanied by TDs movement (*I*).

In the whole process of the $\{10\bar{1}2\}$ TB moving towards the static screw dislocation and then passing it, TDs nucleation and movement play an important role in this TB−dislocation interaction. After the free moving, TB meets the static dislocation. New TD dipoles nucleate steadily at the site where the screw dislocation locates. Subsequently, three individual TDs interact with the original prismatic screw dislocation directly, and convert it to a basal screw dislocation with an extended core.

3.2 Interaction between static $\{10\bar{1}2\}$ TB and moving $1/3\langle 11\bar{2}0\rangle\{10\bar{1}0\}$ prismatic screw dislocation

In this simulation, the $\{10\bar{1}2\}$ TB is kept static, while the $1/3\langle 11\bar{2}0\rangle\{10\bar{1}0\}$ prismatic screw dislocation moves towards it, as shown in Fig. 1(b). The result is significantly different from that of the moving TB model in section 3.1. It can be seen in Fig. 3(*A*−*D*) that the screw dislocation goes through the TB under the shear strain load, converting its slip plane from prismatic to basal. This result is exactly the same as the prismatic-slip−basal-slip (PS-BS) transmission process in metal Ti that SERRA and BACON have described [18].

There are two details which should be mentioned. The first detail is indicated that the original prismatic dislocation temporarily switches to a new prismatic plane after it goes through the TB (*C*). With the increase of the strain, however, this new prismatic dislocation will finally convert to a basal dislocation (*D*). This temporary prismatic dislocation configuration is a transition state from the original prismatic to the basal dislocation. We suppose that this transition state is caused by the complicated local stress environment at the intersection

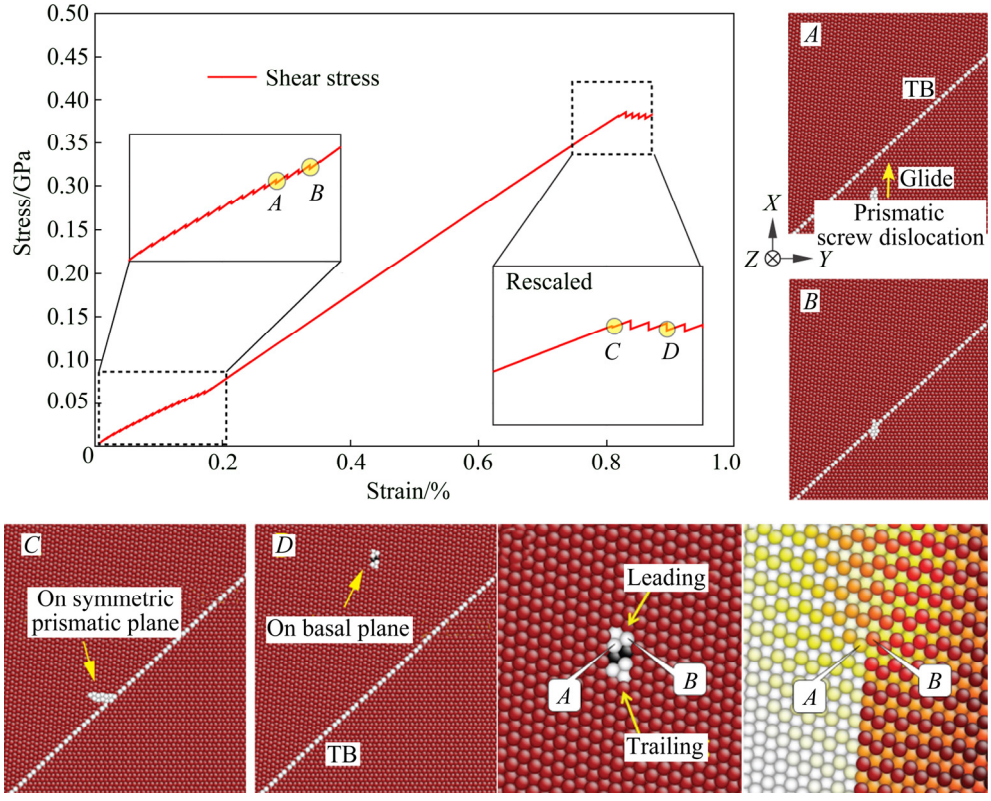

Fig. 3 Stress−strain curve and corresponding atomic configurations of static $\{10\bar{1}2\}$ TB interacting with moving $1/3\langle 11\bar{2}0\rangle\{10\bar{1}0\}$ prismatic screw dislocation (*A*−*D*)

site where the dislocation meets the TB, since the rigid body which applies the shear strain into the system is mainly in the matrix region as shown in Fig. 1(b). Furthermore, as indicated in Fig. 4, although the dislocation meets the TB at the wide space (solid line) as it is reported in Ref. [15], the outgoing slip system in this work merges into narrow glide plane (dash line). The basal dislocation as the product in this work does not follow exactly the rules concluded for Ti and Mg [15].

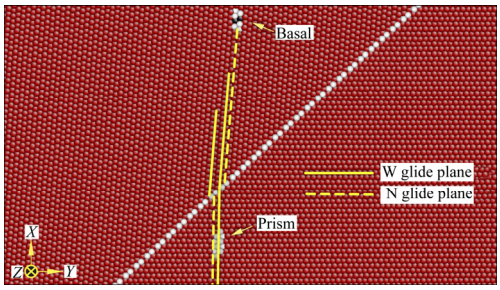

Fig. 4 Comparison of dislocation trajectory

The second detail is the dissociation mechanism of the basal-core dislocation (*E* and *F*). In *E*, we observed that there is a basal stacking fault (SF) between the leading and trailing partial dislocations. From the geometrical analysis, both the leading partial and the trailing partial have screw and edge components. For the leading partial, it is not easy to distinguish the existence of screw components. But if we carefully compare the displacement in $\langle 11\bar{2}0\rangle$ direction between atoms *A* and *B* in *F*, it is still clear that the leading partial indeed separates two atoms away in $\langle 11\bar{2}0\rangle$ direction. The dissociation is described by

$$1/3\langle 11\bar{2}0\rangle \rightarrow 1/3\langle 10\bar{1}0\rangle^{\mathrm{T}} + 1/3\langle 01\bar{1}0\rangle^{\mathrm{T}} \quad (1)$$

where superscript "T" means that the vector is in the twin grain. The length of the basal SF is so short that it merely extends only one lattice constant. Due to the relatively high basal SF energy of 12.4 meV/A^2 for this potential, the energy provided by the external loading is just enough for the dislocation dissociation on the basal plane, incapable of supporting a long SF. From the linear increase of stress between strains 0.2% and 0.8% in Fig. 3, we can tell that driving a prismatic screw dislocation through $\{10\bar{1}2\}$ TB needs a lot of energy. Thus, the dislocation is stuck at the interface during the linear increase of stress. Before the contact, the gliding of screw dislocation reflects itself on the periodical oscillation of strain−stress curve, which is magnified in Fig. 3 where configurations *A* and *B* are also denoted. Because the stress in Fig. 3 is taken from the mean value of the whole system while not from dislocation gliding plane, it continuously goes up as the total elastic strain increases, especially considering the TB and twinning itself as strong inhibition to elastic strain. Therefore, one does not see Peierls stress in Fig. 3. But the calculated stress is still reasonably at the same order of the Peierls tress [30]. Moreover, after the dissociated dislocation on basal plane slipped out the model (after configurations *C* and *D*), the stress increases linearly again when strain is larger than 0.9% (to 0.47 GPa in this figure).

3.3 Interaction between static $\{10\bar{1}1\}$ TB and moving $1/3\langle 11\bar{2}0\rangle\{10\bar{1}0\}$ prismatic screw dislocation

We changed TB from $\{10\bar{1}2\}$ to $\{10\bar{1}1\}$ to see what is different when it interacts with the same screw dislocation as mentioned in section 3.2. Unlike the result of $\{10\bar{1}2\}$ TB, the moving prismatic screw dislocation cannot pass the $\{10\bar{1}1\}$ TB. Instead, it is absorbed and subsequently dissociated into TDs (b, $2h_0$) on the $\{10\bar{1}1\}$ TB (*C* and *D*). This result is consistent with previous researches on other hcp metals [15]. The two TDs nucleated at the interface have the same screw component of Burgers vector of $1/6\langle 11\bar{2}0\rangle$ (*E* in Fig. 5) which is visualized by atom displacements along the dislocation line. But these two TDs also have opposite edge components, which is equal to $1/2\rho^{(\bar{1}011)}\langle\bar{1}01\bar{2}\rangle$, where $\rho^{(\bar{1}011)}$ is a function of c/a as WANG et al stated [27]. With the increasing loading, one of them becomes sessile (*D*). The initial spacing between these two TDs is approximately 9Å, reflecting that the strain energy introduced by the screw dislocation is transformed into the interaction scaled by the corresponding force between these two TDs. Similar to simulations of $\{10\bar{1}1\}$ TB in magnesium and titanium [15, 27], we did not observe (b, $4h_0$) TD either.

Figure 5(a) shows the stress−strain curve of this interaction. Note that the curve does not start from zero stress because the initial defects (screw dislocation) are introduced in the modeling system. This stress−strain curve implies that the interaction between the screw dislocation and the $\{10\bar{1}1\}$ TB does not need such high stress as the screw dislocation interacts with the $\{10\bar{1}2\}$ TB. Actually, the screw dislocation will be absorbed spontaneously within a distance of about 6 Å as proved in Ref. [18], which means that this pure displacive mechanism has little energy barrier to overcome. To determine the barrier of this pure displacive mechanism, we employed nudged elastic band (NEB) [31,32] method to extract two frames from discrete strain load as the initial and final state of the interaction. For a better description of this "stress-driven" process [17,33−35], the final state was unloaded to the same stress environment as the initial state has. The result shown in Fig 5(b) indicates that the barrier is less than 0.05 eV under stress of 0.038 GPa, which is at the same level of system thermal energy of approximately 0.025 eV at 300 K.

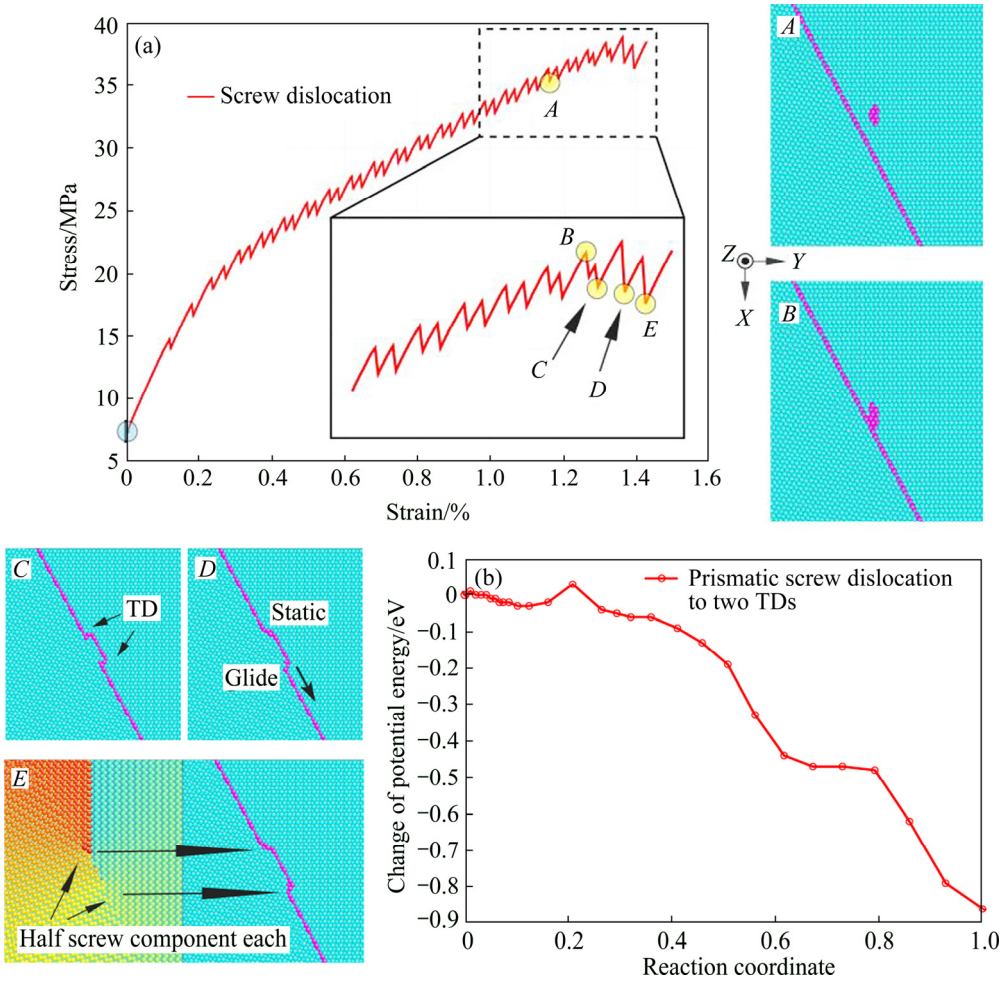

Fig. 5 Stress−strain curve (a), nudged elastic band (NEB) results (b), and corresponding atomic configurations of $\{10\bar{1}1\}$ TB interacting with moving $1/3\langle 11\bar{2}0\rangle\{10\bar{1}0\}$ prismatic screw dislocation (*A*−*E*)

4 Comparison and discussion

As an important part of polycrystalline bulk material plasticity, interactions between dislocations and TBs have been studied. The interaction mechanism we found here when a moving $\{10\bar{1}2\}$ TB interacts with a static screw dislocation is quite interesting, because it reveals the contribution of TDs. Free movement of TB is accomplished by the nucleation and movement of TDs, and total three TDs are involved in the interaction processes. When TB is static and the screw dislocation is moving, the PS−BS transmission is found after the screw passes the TB, which is quite different from the case of a moving TB. From Figs. 6(a, b) we could see the difference between two $1/3\langle 11\bar{2}0\rangle$ basal screw dislocations, separately produced in these two cases. In the moving dislocation case, basal screw dislocation splits into two Shockley partials which are both on the same (0001) plane, as they usually do. In the moving TB case, the two partials of the basal screw dislocation do not lie on the same (0001) plane. They have opposite pyramidal components on $\{10\bar{1}1\}$ plane as shown in Fig. 6.

Figure 7 shows the comparison of stress−strain curves of the moving TB and moving dislocation models for the interactions between the $\{10\bar{1}2\}$ TB and the $1/3\langle 11\bar{2}0\rangle\{10\bar{1}0\}$ prismatic screw dislocation. It can be seen that due to the high mobility of prismatic screw dislocation, the stress threshold of dislocation passing through $\{10\bar{1}2\}$ TB is below 0.4 GPa. Much of the stress needed in the moving-dislocation case is required by the PS−BS transmission when the screw dislocation is stuck at the interface, indicated by the range *A* in Fig. 7. While for the moving-TB case, the energy accumulation from contacting to detaching is apparently much smaller (<0.1 GPa, indicated by range *B* in yellow). The linear increase of the stress to around 0.54 GPa (blue curve) is for TD dipole nucleation on a defect-free TB. In practice, $\{10\bar{1}2\}$ TB would not be defect-free, it always has TDs at the interface or TD nucleation site such as triple junctions. So, the motion of TB could be achieved at

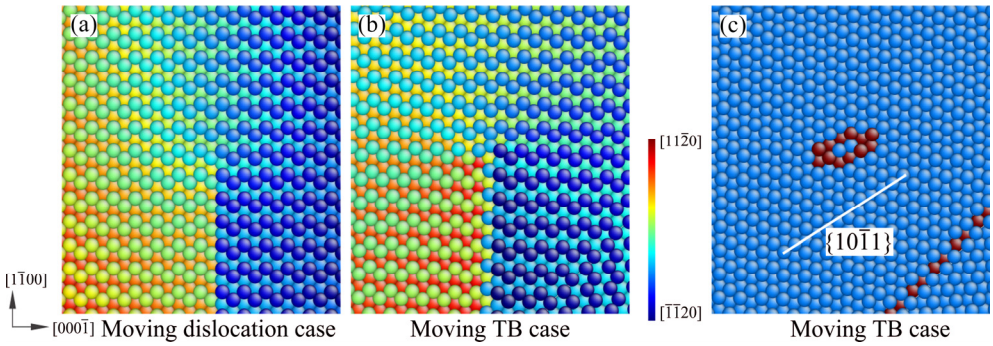

Fig. 6 Displacements along Burgers vector direction of two basal screw dislocations (a, b) and common neighbor analysis of dislocation produced in moving TB case (c)

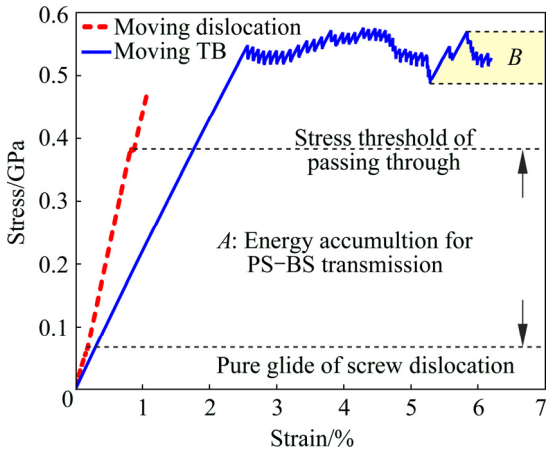

Fig. 7 Comparison of stress−strain curves: moving TB and moving dislocation models for {10$\bar{1}$2} TB and 1/3⟨11$\bar{2}$0⟩{10$\bar{1}$0} prismatic screw dislocation

lower stress than the blue curve as shown in Fig. 7. For {10$\bar{1}$1} TB interacting with the same screw dislocation described in sections 3.3, we could clearly see the pure displacive mechanism when the screw dislocation is absorbed spontaneously by the TB. Particularly, NEB calculation illustrates that the attraction of the TB for the screw dislocation is lying on the extremely small energy barrier of the absorption mechanism.

5 Conclusions

1) For the interaction of a moving {10$\bar{1}$2} TB with a static 1/3⟨11$\bar{2}$0⟩{10$\bar{1}$0} prismatic screw dislocation, the screw dislocation can be finally detached from the moving TB and changed to a basal screw dislocation by successively nucleated TDs. The Burgers vector of the product is the same as the prismatic one. TDs nucleation and movement play an important role in the TBs migration and interaction of TB and dislocation.

2) For the interaction of a static {10$\bar{1}$2} TB with a moving 1/3⟨11$\bar{2}$0⟩{10$\bar{1}$0} screw dislocation, the situation is different. The prismatic screw dislocation converts into a basal one which dissociates into two partial dislocations and an extremely short SF between them. The different results obtained from the moving TB model and the moving dislocation model imply the contribution of the mobile TDs on the interaction mechanism of TB and dislocation.

3) If we change the TB from {10$\bar{1}$2} to {10$\bar{1}$1} in the moving dislocation model, the interaction mechanisms are totally different. The moving 1/3⟨11$\bar{2}$0⟩{10$\bar{1}$0} prismatic screw dislocation is absorbed by the static {10$\bar{1}$1} TB and then dissociated into two TDs left on the TB. The stress−strain curve implies that the interaction between the screw dislocation and the {10$\bar{1}$1} TB does not need such high stress as the screw dislocation interacts with the {10$\bar{1}$2} one. The minimum energy pathway revealed by NEB method demonstrates the attraction between the screw dislocation and the {10$\bar{1}$1} TB.

References

[1] KACHER J, EFTINK B P, CUI B, ROBERTSON I M. Dislocation interactions with grain boundaries [J]. Current Opinion in Solid State and Materials Science, 2014, 18: 227−243.

[2] WEERTMAN J R, FARKAS D, HEMKER K, KUNG H, MAYO M, MITRA R, SWYGENHOVEN H V. Structure and Mechanical Behavior of Bulk Nanocrystalline Materials [J]. Mrs Bulletin, 1999, 24: 44−53.

[3] LIU M, JIANG T, WANG J, LIU Q, WU Z. Aging behavior and mechanical properties of 6013 aluminum alloy processed by severe plastic deformation [J]. Transactions of Nonferrous Metals Society of China, 2014, 24: 3858−3865.

[4] HALL E O. The deformation and ageing of mild steel: III discussion of results [J]. Proceedings of the Physical Society: Section B, 1951, 64: 747.

[5] PETCH N J. The cleavage strength of polycrystals [J]. Iron Steel Inst, 1953, 174: 25−28.

[6] YIN Y F, XU W, SUN Q Y, XIAO L, SUN J. Deformation and fracture behavior of commercially pure titanium with gradient nano-to-micron-grained surface layer [J]. Transactions of Nonferrous Metals Society of China, 2015, 25, 738−747.

[7] LI X, WEI Y, LU L, LU K, GAO H. Dislocation nucleation governed softening and maximum strength in nano-twinned metals [J]. Nature, 2010, 464: 877−880.

[8] DEWALD M P, CURTIN W A. Multiscale modelling of dislocation/grain boundary interactions. II. Screw dislocations impinging on tilt boundaries in Al [J]. Philosophical Magazine, 2007, 87: 4615−4641.
[9] JIN Z H, GUMBSCH P, ALBE K, MA E, LU K, GLEITER H, HAHN H. Interactions between non-screw lattice dislocations and coherent twin boundaries in face-centered cubic metals [J]. Acta Materialia, 2008, 56: 1126−1135.
[10] ZHU T, LI J, SAMANTA A, KIM H G, SURESH S. Interfacial plasticity governs strain rate sensitivity and ductility in nanostructured metals [J]. Proceedings of the National Academy of Sciences of the United States of America, 2007, 104: 3031−3036.
[11] SØRENSEN M R., MISHIN Y, VOTER A F. Diffusion mechanisms in Cu grain boundaries [J]. Physical Review B, 2000, 62: 3658−3673.
[12] WANG J, BEYERLEIN I J. Atomic structures of symmetric tilt grain boundaries in hexagonal close packed (hcp) crystals [J]. Modelling and Simulation in Materials Science and Engineering, 2012, 20: 024002.
[13] ADLAKHA I, BHATIA M A, TSCHOPP M A, SOLANKI K N. Atomic scale investigation of grain boundary structure role on intergranular deformation in aluminium [J]. Philosophical Magazine, 2014, 94: 3445−3466.
[14] YU Q, QI L, MISHRA R K, LI J, MINOR A M. Reducing deformation anisotropy to achieve ultrahigh strength and ductility in Mg at the nanoscale [J]. Proceedings of the National Academy of Sciences, 2013, 110: 13289−13293.
[15] KASCHNER G C, TOME C N, MCCABE R J, MISRA A, VOGEL S C, BROWN D W. Exploring the dislocation/twin interactions in zirconium [J]. Materials Science and Engineering A, 2007, 463: 122−127.
[16] KACHER J, ROBERTSON I M. In situ and tomographic analysis of dislocation/grain boundary interactions in alpha-titanium [J]. Philosophical Magazine, 2014, 94: 814−829.
[17] MROVEC M, ELSAESSER C, GUMBSCH P. Interactions between lattice dislocations and twin boundaries in tungsten: A comparative atomistic simulation study [J]. Philosophical Magazine, 2009, 89: 3179−3194.
[18] SERRA A, BACON D J. Computer simulation of screw dislocation interactions with twin boundaries in HCP metals [J]. Acta Metallurgica Et Materialia, 1995, 43: 4465−4481.
[19] SERRA A, BACON D J, POND R C. Twins as barriers to basal slip in hexagonal-close-packed metals [J]. Metallurgical and Materials Transactions A, 2002, 33: 809−812.
[20] SERRA A, BACON D J. Interaction of a moving $\{10\bar{1}2\}$ twin boundary with perfect dislocations and loops in a hcp metal [J]. Philosophical Magazine, 2010, 90: 845−861.
[21] YUASA M, MASUNAGA K, MABUCHI M, CHINO Y. Interaction mechanisms of screw dislocations with and twin boundaries in Mg [J]. Philosophical Magazine, 2014, 94: 285.
[22] ZHANG Y, DONG Z, WANG J, LIU J, GAO N, LANGDON T. An analytical approach and experimental confirmation of dislocation–twin boundary interactions in titanium [J]. Journal of Materials Science, 2013, 48: 4476−4483.
[23] EL KADIRI H, BARRETT C D, WANG J, TOMÉ C N. Why are twins profuse in magnesium? [J]. Acta Materialia, 2015, 85: 354−361.
[24] YOSHIDA T, YUASA M, MABUCHI M, CHINO Y. Effect of segregated elements on the interactions between twin boundaries and screw dislocations in Mg [J]. Journal of Applied Physics, 2015, 118: 034304.
[25] MENDELEV M I, ACKLAND G J. Development of an interatomic potential for the simulation of phase transformations in zirconium [J]. Philosophical Magazine Letters, 2007, 87: 349−359.
[26] YUE F, OSETSKIY Y N, YIP S, YILDIZ B. Mapping strain rate dependence of dislocation-defect interactions by atomistic simulations [J]. Proceedings of the National Academy of Sciences of the United States of America, 2013, 110: 17756−17761.
[27] WANG J, BEYERLEIN I J, HIRTH J P, TOME C N. Twinning dislocations on $\{\bar{1}011\}$ and $\{\bar{1}013\}$ planes in hexagonal close-packed crystals [J]. Acta Materialia, 2011, 59: 3990−4001.
[28] CAPOLUNGO L, BEYERLEIN I. Nucleation and stability of twins in hcp metals [J]. Physical Review B, 2008, 78 (2): 024117.
[29] WANG J, HIRTH J P, TOMÉ C N. Twinning nucleation mechanisms in hexagonal-close-packed crystals [J]. Acta Materialia, 2009, 57: 5521−5530.
[30] KHATER H A, BACON D J. Dislocation core structure and dynamics in two atomic models of α-zirconium [J]. Acta Materialia, 2010, 58: 2978−2987.
[31] HENKELMAN G, UBERUAGA B P, JÓNSSON H. A climbing image nudged elastic band method for finding saddle points and minimum energy paths [J]. The Journal of chemical physics, 2000, 113: 9901−9904.
[32] NAKANO A. A space–time-ensemble parallel nudged elastic band algorithm for molecular kinetics simulation [J]. Computer Physics Communications, 2008, 178: 280−289.
[33] MISHIN Y, ASTA M, LI J. Atomistic modeling of interfaces and their impact on microstructure and properties [J]. Acta Materialia, 2010, 58: 1117−1151.
[34] YIP S, SHORT M P. Multiscale materials modelling at the mesoscale [J]. Nature Materials, 2013, 12: 774−777.
[35] SILVA E, FÖRST C, LI J, LIN X, ZHU T, YIP S. Multiscale materials modelling: Case studies at the atomistic and electronic structure levels [J]. ESAIM: Mathematical Modelling and Numerical Analysis, 2007, 41: 427−445.

金属锆中螺位错与孪晶界反应的原子模拟

汤笑之，张慧识，郭雅芳

北京交通大学 力学系，北京 100044

摘　要：采用分子静力学模拟密排六方金属锆中孪晶界与螺位错之间的交互作用。在移动晶界模型中，研究一个移动的 $\{10\bar{1}2\}$ 孪晶界与一个静止的 $\langle 11\bar{2}0\rangle$ 螺位错之间的交互作用。在此类交互作用中孪晶位错的形核与移动起到了重要的作用。静止的螺位错穿过了孪晶界并转换为基面上的一个具有宽位错芯的缺陷。在移动位错模型中，一个移动的 $\langle 11\bar{2}0\rangle$ 位错穿过孪晶界并转换为两个基面部分位错及它们之间的一段极短的层错。如果在同一个模型中将孪晶界置换为 $\{10\bar{1}1\}$ 类型，这个移动的 $\langle 11\bar{2}0\rangle$ 柱面螺位错将被完全吸收并分解为孪晶界上的两个孪晶位错。分析相应的应力−应变曲线与缺陷结构，揭示位错与孪晶界之间的复杂交互作用。

关键词：孪晶界；孪晶位错；滑移转换反应；绝热过程

(Edited by Xiang-qun LI)